Journal of Geophysical Research: Biogeosciences

RESEARCH ARTICLE
10.1029/2018JG004649

The Role of Reactive Iron in the Preservation of Terrestrial Organic Carbon in Estuarine Sediments

B. Zhao[1,2,3], P. Yao[1,2], T. S. Bianchi[3], M. R. Shields[3], X. Q. Cui[3,4], X. W. Zhang[3,4], X. Y. Huang[1], C. Schröeder[5], J. Zhao[6], and Z. G. Yu[1,2]

[1]Key Laboratory of Marine Chemistry Theory and Technology, Ministry of Education, Ocean University of China, Qingdao, China, [2]Laboratory for Marine Ecology and Environmental Science, Qingdao National Laboratory for Marine Science and Technology, Qingdao, China, USA, [3]Department of Geological Sciences, University of Florida, Gainesville, FL, USA, [4]Department of Earth, Atmospheric, and Planetary Sciences, Massachusetts Institute of Technology, Cambridge, MA, USA, [5]Biological and Environmental Sciences, School of Natural Sciences, University of Stirling, Stirling, UK, [6]Second Institute of Oceanography, State Oceanic Administration, Hangzhou, China

Key Points:
- Extensive sediment resuspension may reduce reactive iron binding with marine-derived OC
- About 15.6% of sedimentary OC burial is directly associated with reactive iron on a global scale
- The reactive iron plays an important role in stabilization of terrestrial SOC

Supporting Information:
- Supporting Information S1
- Table S1

Correspondence to:
P. Yao,
yaopeng@ouc.edu.cn

Citation:
Zhao, B., Yao, P., Bianchi, T. S., Shields, M. R., Cui, X. Q., Zhang, X. W., et al. (2018). The role of reactive Iron in the preservation of terrestrial organic carbon in estuarine sediments. *Journal of Geophysical Research: Biogeosciences*, *123*, 3556–3569. https://doi.org/10.1029/2018JG004649

Received 12 JUN 2018
Accepted 18 NOV 2018
Accepted article online 3 DEC 2018
Published online 15 DEC 2018

Abstract To better understand the role of reactive Fe (Fe_R) in the preservation of sedimentary organic carbon (SOC) in estuarine sediments, we examined specific surface area, grain size composition, total OC (TOC), lignin phenols, Fe_R, Fe_R-associated OC (Fe-OC) and lignin phenols (Fe-lignin), and $\delta^{13}C$ of Fe_R-associated OC ($\delta^{13}C_{Fe\text{-}OC}$) in surface sediments of the Changjiang Estuary and adjacent shelf. An estimated 7.4 ± 3.5% of the OC was directly bound with Fe_R in the Changjiang Estuary and adjacent shelf. Unusually low TOC/specific surface area loadings and Fe-OC/Fe ratios in mobile muds suggest that frequent physical reworking may reduce Fe_R binding with OC, with selective loss of marine OC. More depleted $^{13}C_{Fe\text{-}OC}$ relative to ^{13}C of TOC ($^{13}C_{bulk}$) in deltaic regions and mobile muds showed that Fe_R was largely associated with terrestrial OC, derived from extensive riverine OC and Fe inputs. A higher proportion of hematite in the mobile muds compared to the offshore samples indicated that Fe oxides are likely subjected to selective sorting and/or become mature during long-term sediment transport. When considering the percentage of Fe-OC to SOC and SOC burial rates in different marine environments (e.g., nondeltaic shelf, anoxic basins, slope, and deep sea), our findings suggest that about 15.6 ± 6.5% of SOC is directly bound to Fe_R on a global scale, which is lower than the previous estimation (~21.5%). This work further supports the notion of a *Rusty Sink* where, in this case, Fe_R plays an important role in the preservation and potential transport of terrestrial OC in the marine environment.

1. Introduction

Organic matter (OM)-mineral interactions can play an important role in the preservation of organic carbon (OC) in marine sediments (Bergamaschi et al., 1997; Burdige, 2005; Hedges & Keil, 1995; Torn et al., 1997). In general, sedimentary OC (SOC) is associated with minerals via mineral surface adsorption, occlusion, the formation of aggregates, and coprecipitation (Keil & Mayer, 2014). The stabilization of SOC through OM-mineral associations is largely influenced by mineral geochemical compositions and environmental conditions (Doetterl et al., 2016). Due to high surface area, reactive iron (Fe_R; defined as the iron phases in sediments which could be extracted by sodium dithionite) is commonly associated with elevated OC (Keil & Mayer, 2014). Fe_R contributes to OC stabilization by isolating from microbial degradation through inner sphere complexation (Barber et al., 2017; Eusterhues et al., 2014; Wagai & Mayer, 2007). Recent work has demonstrated that the binding of OC to Fe_R accounted for ~21.5% of the OC stored in marine sediments (Lalonde et al., 2012). Thus, understanding the mechanisms of OC-Fe associations is important for evaluating long-term storage of OC in marine sediments (Eglinton, 2012; Keil & Mayer, 2014; Lalonde et al., 2012; Shields et al., 2016).

OC associated with Fe_R appears to be more enriched in ^{13}C compared to bulk OC—over a wide range of marine sediments (Lalonde et al., 2012). One particular exception was deltaic sediment from the Mackenzie River Delta, which had a lower $\delta^{13}C$ of Fe_R-associated OC ($\delta^{13}C_{Fe\text{-}OC}$) than bulk OC (Lalonde et al., 2012). Recent work has also shown that Fe_R is associated with more ^{13}C-depleted OC in Wax Lake Delta, in the northern Gulf of Mexico (Shields et al., 2016). Laboratory studies indicate that sorption of terrestrial lignin-derived OC to Al and Fe oxyhydroxides is stronger than more labile polysaccharide-derived OC, because lignin-derived OC has more carboxylic and aromatic carbons which easily complex with Fe_R (Kaiser & Guggenberger, 2000). Consequently, we would expect that a large fraction of the Fe-OC would

have depleted ^{13}C signal, particularly in large-river delta-front estuaries (LDEs) where iron and terrestrial inputs are relatively high (Bianchi & Allison, 2009). Interestingly, the reduction of iron oxides in sediments can break down OC-Fe associations thereby releasing OC back into the system (Adhikari & Yang, 2015; Chen et al., 2015; Chin et al., 1998). Linkhorst et al. (2017) proposed that OC-Fe associations are likely a reversible process and that microbial reduction of iron, triggered by the supply of labile marine OC, may promote the release of terrestrial OC. Moreover, recent work in boreal estuary showed that flocculation of Fe and terrestrial OC was decoupled during sedimentation, resulting in accumulation of labile Fe in the form of ferrihydrite and OC-Fe associations (Jilbert et al., 2018). Clearly, more work is needed to better understand these complex OC-Fe associations in marine sediments, particularly in highly dynamic LDE systems.

The Changjiang (Yangtze) is the largest river in China and carries large quantities of nutrients and sediments to the deltaic region and the adjacent East China Sea (ECS) inner shelf (Milliman et al., 1985; Wu et al., 2007; Zhang, Liu, et al., 2007). These riverine-derived materials are the primary sources of terrestrial OC and Fe_R to deltaic and inner shelf sediments (Lin et al., 2002; Zhu et al., 2012). In large delta-front estuaries, newly deposited fine-grained sediments (silt and clay) often form mobile mud layers that are subject to long-term hydrodynamic sorting and frequent physical reworking activities (Aller, 1998; McKee et al., 2004; Yao et al., 2014; Zhao et al., 2017). Despite high primary production and OC deposition rates in many deltaic regions, the preservation efficiency of OC is relatively low (30%) in mobile muds of the Changjiang Estuary and ECS inner shelf (Blair & Aller, 2012; Yao et al., 2014). In fact, large inputs of Fe oxides, coupled with frequent physical reworking, result in rapid Fe + redox cycling (reduction and reoxidation) which is largely responsible for the loss of SOC in ECS mobile muds (Ma et al., 2018; Yao et al., 2014; Zhao et al., 2017; Zhu et al., 2016). Protracted sediment entrainment in cyclic resuspension-deposition processes can change the properties of SOC, resulting in much lower $\Delta^{14}C$ values (−274‰ to −682‰) on the ECS inner shelf than in suspended OC (−103‰ to −129‰) from the Changjiang Estuary and middle/outer ECS shelf (−174‰ to −280‰; Bao et al., 2016; Van der Voort et al., 2018; Wang et al., 2012). Redox oscillations and transient diagenesis, induced by resuspension in mobile muds, effectively enhance remineralization of SOC; these muds are commonly known as suboxic *fluidized-bed reactors* (Abril et al., 2010; Aller, 1998, 2004; Audry et al., 2007). We posit that the mobile mud belt of the Changjiang LDE is an ideal region for studying OC-Fe associations in sediments largely due to the high inputs of OC and Fe, as well as its fluidized-bed dynamics (Aller, 1998; Yao et al., 2014; Zhao et al., 2017, 2018).

While there have been many studies on the diagenesis and remineralization of SOC in the Changjiang Estuary (e.g., Aller et al., 1985; Yao et al., 2014; Zhao et al., 2017; Zhu et al., 2016), few studies have examined the mechanisms of SOC preservation, especially the role of minerals in the preservation of SOC. In this study, we examined total OC (TOC), stable carbon isotope composition ($\delta^{13}C_{bulk}$), grain-size composition, specific surface area (SSA), Fe_R, Fe_R-associated SOC (Fe-OC), and Fe_R-associated lignin phenols (Fe-lignin) in surface sediments of the Changjiang Estuary and adjacent shelf—in both summer and winter seasons. This work builds on previous studies focused on evaluating the preservation of SOC by Fe_R in different marine environments to better understand the role of OC-Fe associations on a global scale (Lalonde et al., 2012; Ma et al., 2018; Salvadó et al., 2015; Shields et al., 2016).

2. Materials and Methods

2.1. Site Description and Sampling

The study area is located in the Changjiang Estuary and adjacent ECS shelf (Figure 1). The Changjiang has the fourth largest sediment flux (~4.8×10^8 t/year) and fifth greatest water discharge (9.0×10^{11} m^3/year) in the world (Milliman & Farnsworth, 2011). The transport of terrestrial materials, carried by the Changjiang Diluted Water (CJDW), is mainly controlled by the Taiwan Warm Current, Zhe-Min Coastal Current (ZMCC), and the Yellow Sea Coastal Current (Liu et al., 2006, 2007; Figure 1a). The hydrographic regimes of the Changjiang Estuary vary largely on a seasonal basis. In summer, during the prevailing southeast monsoon, the Taiwan Warm Current is intensified and the ZMCC is weakened (Lee & Chao, 2003; Liu et al., 2003). At the same time, large inputs of nutrients from the Changjiang River enhance primary production in summer, resulting in coastal algae blooms and bottom-water hypoxia in the Changjiang Estuary and adjacent inner shelf (Li et al., 2002; Zhao et al., 2015; Zhu et al., 2015). In contrast, under the intensified ZMCC in winter, much of the sediment load of the Changjiang Estuary is transported to the Zhe-Min Coast along the ECS inner shelf

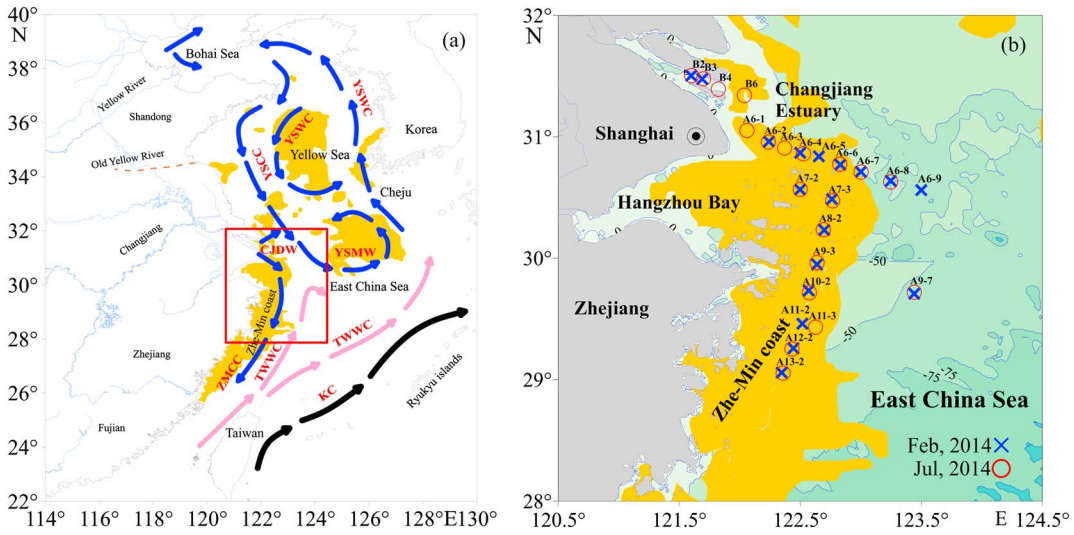

Figure 1. (a) Ocean circulation patterns in the study area. Mud deposits (yellow area) are shown according to Qin et al. (1996). Arrows denote the direction of currents according to Liu et al. (2007). CJDW = Changjiang Diluted Water; ZMCC = Zhe-Min Coastal Current; YSCC = Yellow Sea Coastal Current; YSWC = Yellow Sea Warm Current; YSMW = Yellow Sea Mixing Water; TWWC = Taiwan Warm Current; KC = Kuroshio Current. (b) Locations of sampling sites.

(Guo et al., 2003; Liu et al., 2006, 2007). This complex circulation pattern impedes cross-shelf transport of sediments and facilitates the formation of a long mobile mud belt from the Changjiang Estuary to the Taiwan Strait (Liu et al., 2006, 2003, 2007). Consequently, sedimentation rates from the Changjiang Estuary to the Zhe-Min Coast vary considerably (e.g., from 0.5 to 6.0 cm/year) and generally reflect a decreasing trend southward and seaward (Liu et al., 2006). Frequent physical reworking, coupled with seasonal erosion and redeposition events, results in the southward transport of terrestrial sediments deposited in the Changjiang Estuary along Zhe-Min coast, which promote rapid iron redox cycling in ECS inner shelf (DeMaster et al., 1985; Ge et al., 2017; Yao et al., 2014; Zhao et al., 2017; Zhu et al., 2016).

Two cruises were conducted onboard the *R/V Runjiang 1* in February and July 2014. Thirty-eight surface sediment samples were collected in winter and summer seasons using a Box corer (Table S1 in the supporting information). Surface sediments (0–3 cm in depth) were carefully subsampled by scooping sediments into precombusted small aluminum boxes. Sediments were stored at −20 °C and then freeze dried prior to laboratory analyses. The Changjiang Estuary is characterized by high sedimentation rates (~3 cm/year based on ^{210}Pb data; Liu et al., 2006), with significant seasonal erosion (winter) and redeposition (summer) activities. Thus, we think that he upper 3 cm of sediments likely captures this seasonal variability.

2.2. Sediment Grain Size Composition and Surface Area

Grain size composition was analyzed using a laser Particle Size Analyzer (MS 2000, Malvern, UK; Yao et al., 2014). Particle sizes were separated into the following three groups: clay (<4 μm), silt (4–63 μm), and sand (>63 μm). The relative standard deviation of duplicate samples was less than 3% (n = 6). The SSA was measured using an automatic surface area analyzer (3H-2000PH4, Beishide Instrument-ST Co) after removing OM—based on the static nitrogen-adsorption capacity method.

2.3. Bulk Element and Isotope

TOC and $\delta^{13}C_{bulk}$ in surface sediments were analyzed after removing carbonates by acid fumigation and oven drying at 60 °C for 24 hr (Wang et al., 2015). Measurements were carried out using an elemental analyzer (NA1500, Carlo Erba) interfaced with an isotope ratio mass spectrometer (Delta V Plus, Thermo Scientific) in the Light Stable Isotope Mass Spec Lab, University of Florida. The precision of lab standards (USGS40) was ±0.03% for TOC and ±0.05 ‰ for $\delta^{13}C$ (n = 4).

2.4. Extraction of Fe_R and Fe-OC

Fe_R and Fe-OC were extracted using citrate-dithionite reduction method - according to Mehra and Jackson (1958), as modified by Lalonde et al. (2012). Briefly, sediments (~1 g dry weight) were freeze dried,

homogenized, and then extracted at 80 °C for 15 min in a solution of sodium dithionite, trisodium citrate, and sodium bicarbonate. The resulting suspension was centrifuged for 10 min at 3,000 rpm after extraction and rinsed 3 times with artificial seawater. The supernatant and rinsed water was acidified (pH $<$ 2) and preserved at 4 °C for dissolved Fe analyses. Prior to Fe measurements, these water samples were centrifuged again to remove fine particles. Dissolved Fe in the supernatant and rinsed water was measured on 1:200 diluted aliquots in nitric acid (2%), using inductively coupled plasma mass spectrometry (Element 2, Thermo-Finnigan). The reported analytical uncertainty for dissolved Fe in replicate samples was less than 5%. The residual sediments were freeze dried before analyzing TOC, $\delta^{13}C$, and lignin phenols. A control experiment was carried out before the extraction experiment in the absence of the dithionite reducing agent, to correct for the OC that may have been lost from other extraction effects (pH, ionic strength, physical mixing, heat, etc.). In the control experiment, all sediment samples were extracted under the same protocol but with sodium chloride in place of sodium dithionite. The percentage of Fe-OC to TOC ($f_{Fe\text{-}OC}$) was calculated by the difference of TOC before and after the extraction experiment—$\delta^{13}C_{Fe\text{-}OC}$ values were calculated based on a mass balance calculation (Salvadó et al., 2015; see Text S1 in supporting information).

2.5. Mössbauer Spectroscopy

Selected sediment samples (A6-2W, A6-8W, A6-2S, and A6-8S) were analyzed with a miniaturized Mössbauer spectrometer MIMOS II (Klingelhöfer et al., 2003). Sediment samples in ziplock bags were placed directly on the instrument. Mössbauer spectra were collected at room temperature in backscattering geometry with a ^{57}Co in rhodium matrix radiation source in constant acceleration mode. Spectra were calibrated against a measurement of α-Fe(0) foil (25-μm thickness) at room temperature and evaluated with an in-house fitting routine (Mbfit) using Lorentzian line profiles. Mbfit is based on the least squares minimization routine MINUIT (James, 2004). Since the experiments in this study were all conducted at room temperature, no f-factor was applied. The temperature-dependent f-factor represents the fraction of recoilless transitions to the total number of Mössbauer transitions of the Fe nucleus.

2.6. Analytical Methods for Lignin Phenols

Lignin phenols were extracted and measured in bulk and residue sediments (pre-Fe_R and post-Fe_R extraction) following the method from Hedges and Ertel (1982), as modified by Goñi and Hedges (1995). In short, homogenized freeze-dried sediments containing 3–5 mg of OC were added into stainless steel reaction bombs with 330 ± 4-mg cupric oxide, 106 ± 4-mg ferrous ammonium sulfate hexahydrate, and ~2.5-ml 2 N NaOH solution in a nitrogen glove box. Each bomb was then digested at 150 °C for 3 hr. After which, 50 μl of ethyl vanillin (EVAL) solution (0.5 mg/ml) were added to each bomb as an internal standard. Solutions were neutralized using 6 N HCl and extracted with ethyl acetate 3 times. Sediment samples were derivatized with bis-(trimethylsilyl)-trifluoroacetamide (BSTFA) at 70 °C for 1 hr and analyzed using a gas chromatographer (Trace 1310, Thermo Scientific) interfaced to a triple quadrupole mass spectrometer (TSQ8000, Thermo Scientific).

Quantification of lignin phenols was based on recovery (ethyl vanillin [EVAL] and internal (methyl 3, 4-dimethoxybenzoate) standards, used for calculating relative response factors, and a mix standard of 12 lignin phenols. The mix standard included three vanillyl phenols (V = vanillin [VAL] + acetovanillone [VON] + vanillic acid [VAD]), three syringyl phenols (S = syringaldehyde [SAL] + acetosyringone [SON] + syringic acid [SAD]), two cinnamyl phenols (C = *p*-coumaric acid [CAD] + ferulic acid [FAD]), three *p*-hydroxybenzenes (P = *p*-hydroxybenzaldehyde [PAL] + *p*-hydroxyacetophenone [PON] + *p*-hydroxybenzoic acid [PAD]), and 3,5-dihydroxybenzoic acid (3,5-Bd). The Λ_8 (mg/100 mg OC) is the sum concentration of eight major lignin phenols (S + V + C) normalized to 100 mg of OC. The Σ_8 (mg/g dry sed) is the concentration of above eight major lignin phenols normalized to the weight of dry sediment.

2.7. Calculation of Global Fe-OC Burial Rates

Based on OC burial rates and $f_{Fe\text{-}OC}$ in different marine environments (Hedges & Keil, 1995), we calculated the Fe-OC burial rates and proportion of Fe-OC to SOC to better understand the role of Fe_R in preservation of SOC. The Fe-OC burial rates were calculated using the following equation:

$$\text{Fe} - \text{OC burial rate} = \text{OC burial rate} \times f_{\text{Fe}-\text{OC}} \quad (1)$$

2.8. Statistical Analyses

The SPSS 22 software was used for data analysis. A Pearson correlation analysis with a two-tailed test was used to identify correlations between all measured parameters. Significant statistical differences, based on the 95% confidence intervals, were determined by one-way analysis of variance and a *t* test.

3. Results

3.1. Bulk Properties of Surface Sediments

Bulk properties of surface sediments in the Changjiang Estuary and adjacent shelf are shown in Table S1. The sampling sites were categorized into the following three groups—based on location and water depth: estuarine, mobile muds, and offshore regions (Table S1). The SSA values of surface sediments ranged from 2.82 to 25.8 m^2/g with a mean of 14.0 m^2/g (Standard deviation [SD] = 5.98 m^2/g). The SSA values in mobile muds (17.3 ± 3.29 m^2 g^{-1}) were higher than those in estuarine (6.85 ± 5.24 m^2/g) and offshore regions (6.70 ± 2.09 m^2/g; $p < 0.05$; Table S1). The median grain size ranged largely from 6.8 to 245.7 μm with an average of 38.0 μm (SD = 57.2 μm; Table S1). Relative to mobile muds, higher median grain size values were mainly found in estuarine and offshore regions ($p < 0.05$). Fine-grained sediments (silt and clay) dominated in mobile muds, accounting for more than 80% of total sediment (Table S1). The TOC contents of surface sediments ranged from 0.10% to 0.72%, with a mean of 0.47% (SD = 0.15%). Similar with the distributions of SSA and fine-grained sediments, relatively high TOC contents were mainly found in mobile muds. The $\delta^{13}C_{bulk}$ values ranged from −24.7‰ to −20.4‰ with an average of −22.6‰ (SD = 1.06‰) and were more enriched from the Changjiang Estuary to offshore regions (Table S1). The TOC/SSA loadings of surface sediments ranged from 0.25 to 0.73 mg/m^2, with an average of 0.37 mg/m^2 (SD = 0.12 mg/m; Table S1). Distinctly low TOC/SSA loadings were mainly found in the mobile muds (<0.4 mg/m^2), which supported previous work (Yao et al., 2014). There were no significant differences in bulk properties between summer and winter ($p > 0.05$), which is likely because mixing in surface sediments by physical reworking activities in both summer and winter (DeMaster et al., 1985; Yao et al., 2014; Zhao et al., 2017).

3.2. OC-Fe Associations

The Fe_R, $f_{Fe\text{-}OC}$, $\delta^{13}C_{Fe\text{-}OC}$, and Fe-OC/Fe ratios in surface sediments of the Changjiang Estuary and adjacent shelf are shown in Table S2. The Fe_R contents ranged from 45.6 to 213.8 μmol/g sed with a mean of 133.3 μmol/g sed (SD = 45.5 μmol/g sed). The Fe_R contents in offshore sediments ranged from 45 to 70 μmol/g sed, which was similar to previous findings in the ECS (Ma et al., 2018). The $f_{Fe\text{-}OC}$ of surface sediments varied from 1.89% to 18.8%, with an average of 7.41% (SD = 3.52%). Significantly lower $f_{Fe\text{-}OC}$ values were mainly found in mobile muds (6.13 ± 2.07%) relative to estuarine regions (11.3 ± 3.58%) ($p < 0.05$). For offshore regions, the $f_{Fe\text{-}OC}$ varied largely from 2.5% to 18.75%, with an average of 9.38 ± 5.11%, which was likely affected by seasonal variations and/or uncertainties of sampling, especially in some intermediate sites between two different regions (e.g., A6-7S and A6-7W). The $\delta^{13}C_{Fe\text{-}OC}$ values ranged from −37.7‰ to −16.2‰ (mean = −27.3 ± 5.57‰), with significantly more depleted $^{13}C_{Fe\text{-}OC}$ in estuarine (−24.2 ± 1.23) and mobile mud sediments (−29.8 ± 4.66) than offshore regions ($p < 0.05$). The Fe-OC/Fe molar ratios in surface sediments ranged from 0.05 to 0.73 with a mean of 0.23 (SD = 0.14). Similar to the distribution pattern of $f_{Fe\text{-}OC,}$ significantly lower Fe-OC/Fe molar ratios were mainly found in mobile muds ($p < 0.05$), near the Changjiang Estuary. Similar to bulk properties, there were no significant differences between two seasons for $f_{Fe\text{-}OC,}$ $\delta^{13}C_{Fe\text{-}OC}$, and Fe-OC/Fe ratios ($p > 0.05$).

3.3. Mössbauer Spectroscopy

Mössbauer spectra were obtained from mobile mud samples (station A6-2) and offshore samples (station A6-8) collected at two different seasons. Iron was present as Fe^{2+} in octahedral coordination and Fe^{3+} distributed between (super) paramagnetic phase(s) and hematite (Fe_2O_3). The ferrous phase could be a clay mineral or other silicate phase. The ferric Fe in the (super) paramagnetic fraction can include iron (oxyhydr) oxides, such as ferrihydrite, akaganéite (β-FeOOH), lepidocrocite (γ-FeOOH), (super) paramagnetic goethite (α-FeOOH), and hematite indicating particle sizes <30 nm, and ferric iron in a clay mineral or other silicate phase. Fe_R is expected to be proportional to this (super) paramagnetic Fe^{3+} fraction which is dominant in all samples (Table S3). The offshore samples contained a higher fraction of ferrous Fe compared to the mobile mud samples (Table S3 and Figure S1), independent of season. There was no significant difference between

seasons in the offshore samples. The ferrous fraction in mobile mud samples was not significantly different, but the fraction of ferric iron in hematite was significantly larger in summer compared to winter.

3.4. Lignin Phenols

The lignin phenols and related parameters in bulk sediments are shown in Table S4. The Σ_8 of surface sediments ranged from 7.9 to 172.5 μg/g sed, with a mean of 51.5 μg/g sed (SD = 36.0 μg/g sed). For OC normalized lignin phenols, Λ_8 ranged from 0.23 to 2.92 mg 100 mg^{-1} OC, with an average of 1.20 mg 100 mg^{-1} OC (SD = 0.63 mg 100 mg^{-1} OC). Both Σ_8 and Λ_8 decreased significantly from the Changjiang Estuary to offshore sites. There were two major categories of lignin-related parameters: reflective of sources and degree of lignin phenol degradation. The weight ratios of C to V (woody/nonwoody) and S to V (gymnosperm/angiosperm) are used to identify sources of lignin-derived OC, with higher C/V ($>$ 0.35) and S/V ($>$ 0.80) commonly associated with nonwoody angiosperms (Hedges & Mann, 1979). The C/V and S/V ratios ranged from 0.13 to 0.70 and 0.66 to 1.24, with averages of 0.26 (SD = 0.14) and 0.85 (SD = 0.12), respectively, which indicated a primary mixture source of woody/nonwoody angiosperms. The acid-to-aldehyde weight ratios of V (VAD/VAL, $(Ad/Al)_V$) and S (SAD/SAL, $(Ad/Al)_S$) lignin phenols have been used to indicate the degree of lignin degradation (Hedges et al., 1988). The $(Ad/Al)_V$ and (Ad/Al) s in bulk sediments ranged from 0.23 to 1.21 and 0.28 to 1.04, with averages of 0.57 (SD = 0.21) to 0.51 (SD = 0.18), respectively. The 3,5 Bd/V ratio, which is considered to be an indicator of oxidation of OC in soils (Houel et al., 2006; Louchouarn et al., 1999), ranged from 0.03 to 0.34, with a mean of 0.11 (SD = 0.08). The P/(S + V) ratio is used to indicate degradation state of lignin side chains by brown-rot fungi (Dittmar & Lara, 2001), based on the premise that demethoxylation results in selective loss of the OCH_3 group in S and V families and not in the *p*-hydroxyphenols (Hedges & Ertel, 1982). The P/(S + V) weight ratios ranged from 0.11 to 0.84 with an average of 0.27 (SD = 016). All the lignin-related parameters, indicative of the degree of lignin degradation, increased from the Changjiang Estuary to offshore regions, indicating that the degradation of lignin-derived OC was continuous along the sediment dispersal pathway (Li et al., 2014).

The lignin phenols and related parameters in the Fe_R extracted sediments (after Fe_R extraction) are shown in Table S5. The Σ_8 in Fe_R extracted sediments ranged from 4.2 to 103.2 μg/g sed., with a mean of 38.7 μg/g sed (SD = 22.3 μg/g sed), and Λ_8 ranged from 0.26 to 2.81 mg 100 mg^{-1} OC, with an average of 0.93 mg 100 mg^{-1} OC (SD = 0.53 mg 100 mg^{-1} OC). OC-normalized lignin phenols decreased significantly after Fe_R extraction (Λ_8; $p < 0.05$). The C/V and S/V ratios ranged from 0.13 to 0.53 (mean = 0.33 ± 0.08) and 0.40 to 1.00 (mean = 0.85 ± 0.15), respectively, which are comparable to those in bulk sediments. The $(Ad/Al)_V$ and (Ad/Al) s in residue sediments ranged from 0.14 to 0.61 and 0.27 to 0.63, respectively, with averages of 0.44 (SD = 0.10) and 0.42 (SD = 0.09), respectively. The 3,5-Bd/V ranged from 0.01 to 0.22 with a mean of 0.07 (SD = 0.04). The P/(S + V) ranged from 0.08 to 0.49 with an average of 0.20 (SD = 0.08). All parameters indicative of degree of lignin degradationin in Fe_R extracted sediments were significantly lower than in bulk sediments ($p < 0.05$; Table S5).

It is important to note that while a fraction of the SOC dissolved in the control experiment (~8%), the average $\delta^{13}C$ value of the SOC after the control experiment ($\delta^{13}C_{control} = -22.7 \pm 0.97‰$) was not significantly different from bulk sediments ($-22.6 \pm 1.06‰$). Thus, we assumed that lignin was minimally disturbed by dissolution in the control experiment. Recent studies showed that sorption to Fe_R may reduce the yield of lignin phenols using CuO oxidation method (Hernes et al., 2013; Wang et al., 2017), and thus, our estimate of Fe-lignin is possibly underestimated.

4. Discussion

4.1. Fe_R and OC Relationships in the Changjiang Estuary and Adjacent Shelf

Significantly more depleted $f_{Fe\text{-}OC}$ values in mobile muds than in estuarine regions ($p < 0.05$) suggest that OC-Fe associations were unstable and/or not formed in mobile muds—even with relatively high contents of Fe_R and TOC (Figure 2). Higher Fe_R, TOC, SSA, and clay in mobile muds, coupled with significant positive correlations among these bulk parameters, indicated that fine-grained sediments with high contents of Fe_R and TOC were mainly deposited in ECS mobile muds (Figures 2 and S2). Even though ECS mobile muds have high sedimentation rates and inputs of OC from phytodetritus from local shelf production, SOC is not well preserved due to frequent physical reworking (Li et al., 2014; Xu et al., 2015; Yao et al., 2014;

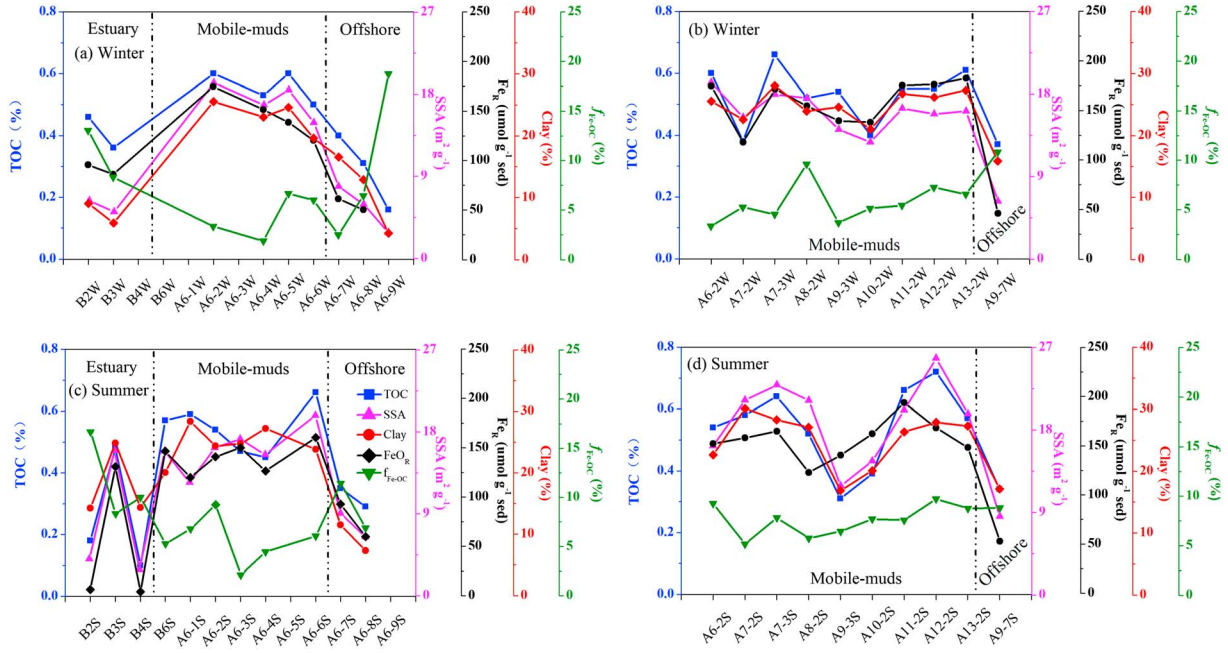

Figure 2. Variations of bulk properties in surface sediments from the Changjiang Estuary to ECS shelf during (a, b) winter and (c, d) summer. ECS = East China Sea; TOC = total organic carbon; SSA = specific surface area.

Zhao et al., 2017). The TOC/SSA ratios (<0.4 mg/m^2) in ECS mobile muds were similar with those in mobile muds of the Amazon-Guianas coastline and Gulf of Papua, showing considerable loss of OC (Figure 2 and Table S2; Aller & Blair, 2006; Aller, Hannides, et al., 2004; Blair & Aller, 2012). A significant positive relationship between TOC/SSA loadings and Fe-OC/Fe ratios indicated that Fe-OC was also partly decomposed due to frequent physical reworking in mobile muds (Figure 3).

Intense remineralization in estuarine mobile muds is generally associated with rapid iron redox cycling (Aller, 2004; Aller, Hannides, et al., 2004, Aller, Heilbrun, et al., 2004; Burdige, 2006; Zhu et al., 2016). Interestingly, despite the overall oxidative environments created by frequent mixing in mobile muds, microenvironments within particle aggregates allow for suboxic reactions (e.g., Fe reduction) to occur (Wells et al., 1995). Past work has shown that frequent physical reworking and large inputs of reactive Fe oxides near the Changjiang Estuary promote the iron reduction—with suppression of sulfate reduction (Liu et al., 2014; Zhao et al., 2017, 2018; Zhu et al., 2012, 2016). In fact, authigenic nonsulfidized Fe (II) are the dominant phases in ECS mobile muds, suggesting the prevalence of iron redox cycling in these sediments (Zhu et al., 2016). Thus, it seems likely that frequent physical reworking of particles in mobile muds accelerates iron cycling and further enhances remineralization of SOC (Aller, 2004; Aller, Hannides, et al., 2004, Aller, Heilbrun, et al., 2004; Burdige, 2006). Several laboratory studies have demonstrated that OC-Fe associations are disrupted during microbial iron reduction, which allows for Fe-OC to be released (Adhikari & Yang, 2015; Adhikari et al., 2017). Rates of chemical dissolution of Fe (III) in soils and sediments are highly variable due, in part, to differences in mineralogy, crystallinity, grain size, and impurity content (Hyacinthe et al., 2006). Such mineralogical differences also impact dissimilatory Fe (III) reduction by iron reducers (Roden, 2004). Interestingly, our Mössbauer results showed a lower proportion of ferrous Fe and higher proportion of hematite in the mobile muds compared to the offshore samples (Table S3). In general, hematite, mainly formed in soils, is a more stable, mature, and higher density mineral, compared to those more commonly precipitated in these

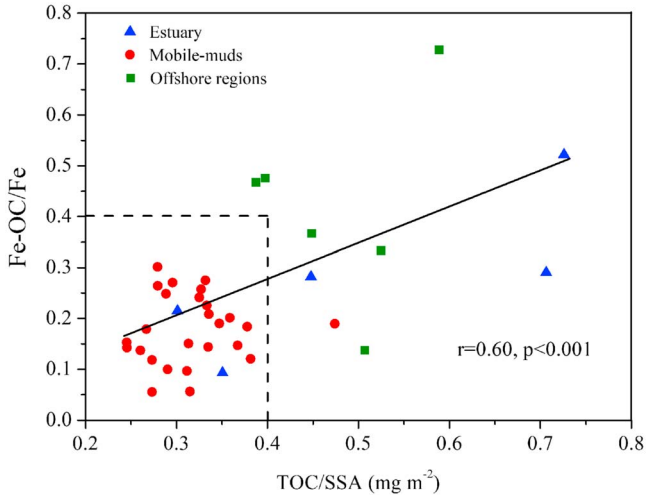

Figure 3. Correlation of the TOC/SSA loadings and Fe-OC/Fe molar ratios in surface sediments of the Changjiang Estuary and adjacent shelf. TOC = total organic carbon; SSA = specific surface area.

estuarine sediments, such as ferrihydrite (Jaynes & Bigham, 1986; Raiswell, 2011). Thus, we hypothesize that the hydrodynamic sorting of riverine-derived sediments leads to the deposition of high-density, crystalline phases such as hematite near the Changjiang Estuary (e.g., A6-2), while low density, poorly crystalline iron oxides such as ferrihydrite are transported to south and offshore regions (Jaynes & Bigham, 1986). Alternatively, the higher proportion of hematite in the mobile muds could be due to the maturation of Fe oxides that experience long-term resuspension and redeposition cycles before eventual burial (Raiswell, 2011; Stucki et al., 2007). Recently, Sirois et al. (2018) proposed that oxidation-reduction oscillations likely enhance Fe_R binding with terrestrial-derived DOC; however, they also argued that the OC-Fe association is likely a transient sink for OC—due to microbial reduction of iron. Our results supported this hypothesis that frequent physical reworking coupled with rapid iron redox cycling in mobile muds is likely removing part of Fe-OC.

The $f_{Fe\text{-}OC}$ (7.4 ± 3.5%) in the Changjiang Estuary and adjacent shelf was comparable to those at the Young site (relative short time since the area became subaerial) of Wax Lake Delta (~8.1%) and the Mackenzie River Delta (7.6%) but lower than the global average (~21.5%; Lalonde et al., 2012; Shields et al., 2016). Moreover, the Fe-OC/Fe ratios in these deltaic regions (Fe-OC/Fe ratio < 1) were also lower than reported for other marine environments (average Fe-OC/Fe ratio = 4.0 ± 2.8; Lalonde et al., 2012). Considering this highly dynamic sedimentary environment near the deltaic region, it seems unlikely that all these OC-Fe associations are formed postdepositionally. In fact, past works showed that some of the binding occurred within the drainage basin and soils before it reaches the deltaic region (Poulton & Raiswell, 2005; Shields et al., 2016). For example, Poulton and Raiswell (2005) found significant relationships between OC and Fe_R in riverine particles and bed sediments, which indicated that OC-Fe associations are likely important for carbon stabilization within drainage basins. Based on our results, we propose that even with the typically large OC and Fe inputs to deltaic sediments, highly dynamic mobile mud environments can reduce the Fe_R binding potential with OC. Further work is clearly needed to better constrain OC-Fe associations in different deltaic regions with varied mixing regimes, sources of OC and mineral surfaces, and a broader range of source rocks and ages in different drainage basins.

4.2. Selective Binding of OC by Fe_R in ECS Mobile Muds

$^{13}C_{Fe\text{-}OC}$ was more enriched than $^{13}C_{bulk}$ in the Changjiang Estuary and mobile muds, than offshore sediments, indicating a preference for binding with terrestrially derived OC in these regions (Figure 4). This agrees with previous work which showed a more depleted $^{13}C_{Fe\text{-}OC}$ for LDE sites, which have higher terrestrially derived inputs (e.g., Mackenzie River Delta and Wax Lake Delta) than nonriver dominated coastal sites with high marine inputs (Lalonde et al., 2012; Shields et al., 2016). The most depleted $\delta^{13}C_{Fe\text{-}OC}$ values in the ECS mobile muds were mainly found in sites with high inputs of terrestrially derived OC (e.g., A6-4W and A8-2S; Li et al., 2014; Yao et al., 2015). This is consistent with notion that Fe_R preferentially binds with more ^{13}C depleted compound classes, such as lipids, cellulose, and lignin (Benner et al., 1987; Meyers, 1997; Shields et al., 2016). Interestingly, the $^{13}C_{Fe\text{-}OC}$ signature was more enriched in the estuarine regions, within the range of phytoplankton and terrestrially derived OC sources, compared to mobile muds, which were more exclusively terrestrially derived. This may suggest that while some of the OC-Fe associations likely occurred in the drainage basin prior to deposition in the estuary, some were made in situ with phytoplankton derived OC. However, as this material is transported to mobile mud belts on the inner shelf, it appears that the phytoplankton signature is lost and the terrestrially derived signature is retained (Figure 4). It may be that the OC-Fe associations formed within the drainage basin are transported to deltaic regions, where this dynamic sedimentary environment inhibits Fe_R binding with more ^{13}C enriched marine-derived OC produced in situ. In addition, the ^{13}C enriched Fe-OC from the Changjiang Estuary was likely preferentially decomposed during postdepositional activities (Figure 4). This rationale agrees well with a recent study in a Fe-rich sandy beach that received large inputs of fresh marine OC, which was rapidly decomposed and resulted in reducing conditions, thereby decreasing the potential Fe_R trapping (Sirois et al., 2018). When Fe oxides are formed at redox interfaces, such as sediment-water interface, it appears that terrestrial-derived OC is preferentially retained by Fe_R, allowing Fe_R to serve as a selective barrier (e.g., Rusty Sink) for the transport of terrestrial OC from the coastal to open ocean (Riedel et al., 2013). However, at sites further offshore from the mobile muds, which is more influenced by the dominant marine OC pool, we see the marine signature return. In fact, much of the OC-Fe associations in mobile muds would be expected to be transported

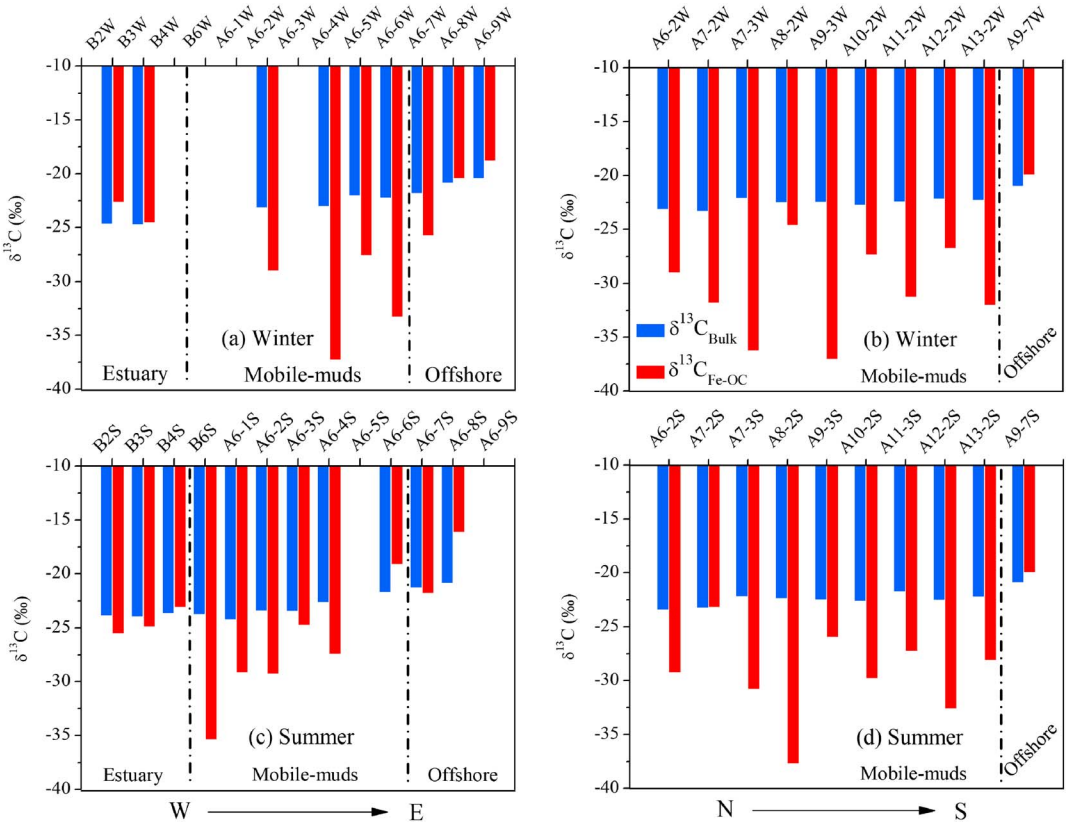

Figure 4. The distributions of $\delta^{13}C_{Bulk}$ and $\delta^{13}C_{Fe\text{-}OC}$ in surface sediments of the Changjiang Estuary and adjacent shelf during (a, b) winter and (c, d) summer.

south within the inner shelf and not offshore to deeper water, due to shearing effects from coastal currents (Li et al., 2014; Xu et al., 2015; Yao et al., 2014).

Although the $f_{Fe\text{-}OC}$ is low (about 7.4% in study area), there are about 27% of bulk lignin phenols (Λ_8, Fe-lignin/bulk lignin) binding with Fe_R, further demonstrating that Fe_R is preferentially bound with terrestrial-derived OC (Tables S3 and S4). This further supports that terrestrially derived OC is preferentially retained in the mobile muds over marine OC—which appears to be lost during transport. Recent laboratory work showed that aromatic, lignin-derived, and carboxylic compounds were preferentially adsorbed to Fe_R (Chen et al., 2014; Linkhorst et al., 2017; Lv et al., 2016). Vascular plant-derived aromatic and pyrogenic compounds in dissolved OM (DOM) appear to be preferentially bound to Fe-oxyhydroxides, in contrast to carboxyl-rich aliphatic acids—which largely remained in solution (Christl & Kretzschmar, 2007; Riedel et al., 2012, 2013). Thus, the dynamic sedimentary environments in the mobile muds will likely lead to more lignin phenols binding with Fe_R. It is worth noting that the lignin-related degradation parameters ($(Ad/Al)_V$, $(Ad/Al)_S$, 3,5-Bd/V and P/(S + V)) in Fe_R extracted sediments were much lower than those in bulk sediments, showing selective adsorption of acidic lignin phenols (e.g., SAD, VAD, CAD, and 3, 5-Bd; Figure 5). A recent study on properties of OC-Fe associations formed from adsorption versus coprecipitation showed that there is ligand exchange between carboxyl functional groups and Fe_R under both formation mechanisms (Chen et al., 2014). Shields et al. (2016) demonstrated that Fe_R preferentially retained acidic lignin phenols at low Fe-OC/Fe ratios in the Wax Lake Delta. Thus, it appears that the $\delta^{13}C_{Fe\text{-}OC}$ signature in the estuarine region is derived from both phytoplankton and terrestrially derived OC and that marine component is preferentially lost during transport to the mobile mud belt on the inner shelf.

4.3. The Preservation of OC in Different Marine Environments by Fe_R

The TOC/SSA loadings, coupled well with Fe-OC/Fe ratios in different marine environments (r^2 = 0.89, $p < 0.001$), indicate that different sedimentary environments influence not only the sorption of OC to

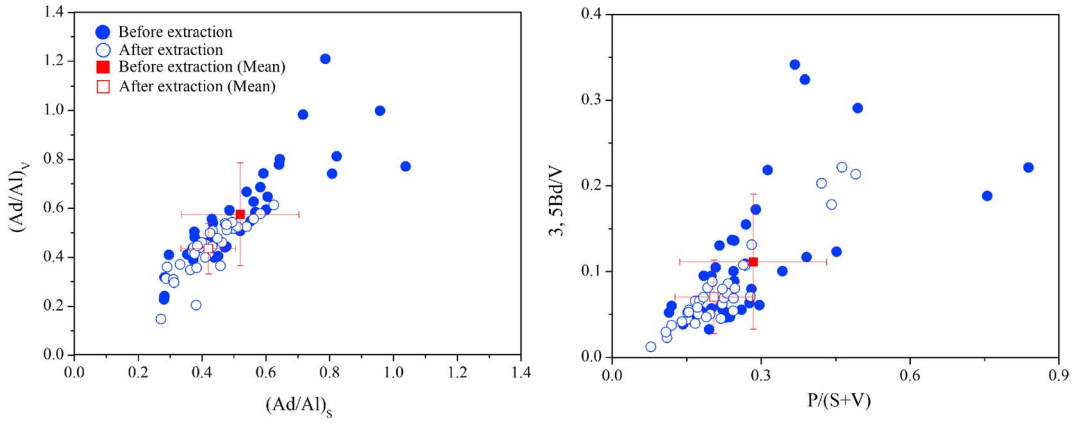

Figure 5. The relationships between (left) $(Ad/Al)_V$ versus (Ad/Al)s and (right) 3,5-Bd/V versus P/(S + V) in the bulk and Fe_R extracted sediments of the Changjiang Estuary and adjacent shelf.

sediment surfaces but also the Fe-OC (Figure 6). In deltaic environments, inputs of riverine Fe-OC and high sedimentation rates lead to burial of Fe-associated terrestrial OC. At the same time, highly dynamic environments (e.g., estuarine mobile muds) prevent Fe_R binding with more OC and even result in loss of Fe-associated marine OC during sediment transport, with more Fe-associated terrestrial OC potentially being retained in mobile muds—due to preferential binding. It is important to note that OC-Fe associations may also greatly influence DOM cycling, especially at the land-sea interface in estuarine regions (Linkhorst et al., 2017; Riedel et al., 2013; Sirois et al., 2018). A recent study in a subterranean estuary showed that terrestrial DOM preferentially flocculated with iron, which led them to believe that subterranean estuaries can also behave as a transient sink of terrestrial OC (Linkhorst et al., 2017). This supports our findings which showed that $\delta^{13}C_{Fe\text{-}OC}$ values were more depleted along a gradient from the Changjiang Estuary to mobile muds of the ECS inner shelf (Figure 4). Moreover, the DOM and newly formed Fe oxides could be continually produced during intense remineralization of SOC in mobile muds (Zhao et al., 2017, 2018; Zhu et al., 2016), and thus, large amounts of terrestrial DOM binding with Fe_R would be expected. Thus, Fe_R plays an important role in stabilization of terrestrial OC in estuarine regions. In nondeltaic shelf regions, Fe_R is binding with marine OC due to high primary production, and Fe-OC is well preserved in nondeltaic sediments because of relatively stable sedimentary environments. In deep-sea environment, long-time deposition resulted in low TOC/SSA loadings, which are comparable to those in mobile muds (Aller & Blair, 2006; Mayer, 1994). However, the Fe-OC/Fe ratios and $f_{Fe\text{-}OC}$ in deep-sea environment are higher than those in mobile muds, indicating that Fe_R also plays an important role in the preservation of OC in deep-sea environment (Figure 6). As mentioned above, the breakdown of OC-Fe associations is likely associated with rapid Fe redox cycling in sediments. Based on a reaction-transport model on a global scale, Thullner et al. (2009) suggested that about 70% of iron reduction occurred in deltaic and inner shelf environment; however, only <10% of iron reduction occurred in slope and deep-sea environment. In addition, there is increasing evidence that rapid iron cycling is largely responsible for the loss of OC in deltaic and mobile muds (Aller, Hannides, et al., 2004, Aller, Heilbrun, et al., 2004; Canfield et al., 1993; Zhu et al., 2016). Thus, rapid redox Fe cycling in deltaic environment likely decomposes the OC-Fe associations as a transient Rusty Sink of terrestrial OC and relatively weaker iron cycling in other environments that facilitate long-term stabilization of Fe-OC.

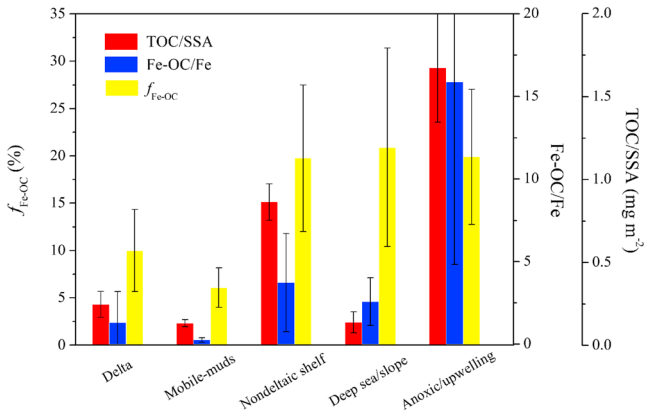

Figure 6. The TOC/SSA loadings, Fe-OC/Fe ratios, and $f_{Fe\text{-}OC}$ in different marine environments. The TOC/SSA ratios are from Aller (1998) and Yao et al. (2014). The Fe-OC/Fe ratios and $f_{Fe\text{-}OC}$ are from Lalonde et al. (2012), Ma et al. (2018), Salvadó et al. (2015), Shields et al. (2016), and this study. Deltaic regions included the Changjiang delta (including mobile muds and shelf), Makenzie river delta, and the Wax Lake Delta (Lalonde et al., 2012; Shields et al., 2016; and this study). Mobile muds included the ECS mobile muds (this study); nondeltaic shelf regions included the Mexican Margin, Madeira turbidite, Arabian Sea, Eurasian Arctic Shelf, middle and outer shelf of ECS, and South Yellow Sea (Lalonde et al., 2012; Ma et al., 2018; Salvadó et al., 2015). Deep Sea/slope regions included the Southern Ocean, Equatorial Pacific, and Station M (Lalonde et al., 2012). Anoxic/upwelling regions included the Black Sea, Mexican Margin, Indian Margin, Lake Brock, and Saanich Intlet (Lalonde et al., 2012). TOC = total organic carbon; SSA = specific surface area.

Table 1
The Burial Rates of Fe-Associated SOC (10^{12}g C/year) in Different Marine Environments

Marine environment	Deltaic	Nondeltaic shelf	Anoxic/upwelling	Slope/deep sea	Total
SOC burial rates[a]	70	74	1	15	160
$f_{Fe\text{-}OC}$[b] (%)	10.0 ± 4.3	19.8 ± 7.7	19.9 ± 7.1	20.9 ± 10.5	—
Fe-OC burial rate	7.0 ± 3.0	14.6 ± 5.7	0.2 ± 0.1	3.13 ± 1.6	24.9 ± 10.4

Note. SOC = sedimentary organic carbon; OC = organic carbon.
[a]The SOC burial rates are from Hedges and Keil (1995). [b]The average $f_{Fe\text{-}OC}$ values of different marine environments are applied in the calculation (for details of different marine environments see caption of Figure 6; data are from Lalonde et al., 2012; Ma et al., 2018; Salvadó et al., 2015; Shields et al., 2016, and this study).

Based on $f_{Fe\text{-}OC}$ and SOC burial rates in different marine environments, we suggest that about 15.6 ± 6.5% of SOC (24.9 ± 10.4 × 10^{12} g C/year) buried in surface sediments is associated with Fe_R on a global scale (Table 1). It was estimated that 21.5 ± 8.6% of the SOC in marine sediments is directly bound to Fe_R (Lalonde et al., 2012). Nevertheless, the generalized percentage of OC associated with Fe in previous study may have overestimated the role of Fe_R in preserving SOC in marine systems (Lalonde et al., 2012). In fact, large inputs of nutrients and terrestrial materials carried by rivers promoted primary productivity and thus resulted in higher OC burial rates in deltaic environments (Bianchi & Allison, 2009; Burdige, 2005; Hedges & Keil, 1995). However, only about 10% of SOC buried in delta and adjacent shelf is associated with Fe_R even with some of the highest OC burial rates in the global ocean (Figure 6). Consequently, high SOC burial rates coupled with low $f_{Fe\text{-}OC}$ showed that a large fraction of the buried SOC in deltaic sediments is not associated with Fe_R. Despite the low proportion of SOC associated with Fe_R, most of the Fe-OC in deltaic environments is derived from land (as well as deltaic wetland erosion), which are important sources of terrestrial OC (Li et al., 2011; Zhang, Wu, et al., 2007). In addition, preferential loss of the marine signal of Fe-OC was also observed in estuarine mobile muds during sediment transport (Figure 4). Consequently, our study suggests that OC-Fe associations play an important role in stabilization of terrestrial SOC in estuarine regions.

5. Conclusions

In summary, the $f_{Fe\text{-}OC}$, TOC/SSA loadings, and Fe-OC/Fe ratios in ECS mobile muds were lower than estuarine regions. This is likely because frequent physical reworking inhibited Fe_R binding with OC and even promoted decomposition of Fe-associated marine OC. In addition, these physical activities such as resuspension and redeposition activities could break the OC-Fe associations through accelerating iron redox cycling in mobile muds. During long-term hydrodynamic sorting processes of sediments, relatively high density of riverine-derived hematite is likely deposited in mobile muds of the ECS inner shelf, resulting in higher proportion of hematite in the mobile muds compared to the offshore samples. Alternatively, Fe oxides also could become mature with a change in the dominant mineral form prior eventual burial.

OC-Fe associations are likely formed during transport from the Changjiang Estuary to ECS mobile muds, resulting in Fe_R bound with more ^{13}C depleted terrestrial SOC. However, Fe_R is associated with ^{13}C enriched OC in offshore regions. Large amounts of Fe-associated terrestrial OC were buried in deltaic regions, and thus, OC-Fe associations limit the transport of terrestrial OC from river to open ocean, consistent with the rusty sink and iron curtain hypotheses (Eglinton, 2012; Lalonde et al., 2012; Linkhorst et al., 2017).

The binding of Fe_R and OC exhibited significant differences in different marine environments, which is largely associated with different sedimentary properties. Globally, there are 15.6 ± 6.5% of SOC (24.9 ± 10.4 × 10^{12} g C/year) buried in marine environment through binding with Fe_R. Most of Fe-OC in deltaic environment is derived from land with preferential loss of the marine signal of Fe-OC during sediment transport. Thus, we conclude that Fe_R plays an important role in stabilization and transport of terrestrial SOC in marine sediments.

Acknowledgments
This study was supported by the National Natural Science Foundation of China (41620104001, 41676063, and 41521064), the 111 project (B13030), and the Creative Team Project of the Laboratory for Marine Ecology and Environmental Science, Qingdao National Laboratory for Marine Science and Technology (LMEES-CTSP-2018-2). We thank the crews of the *R/V Runjiang 1* for sampling assistance. We also thank Jason Curtis and George Kamenov for their analytical supports. Finally, this manuscript was greatly improved, thanks to Editor Miguel Goñi, Tom Jilbert, and another anonymous reviewer for their constructive suggestions and insightful comments. This is MCTL contribution 86. The data used are listed in the supporting information. Supporting information data to this article can be found online at https://doi.org/10.1029/2018JG004649.

References

Abril, G., Commarieu, M. V., Etcheber, H., Deborde, J., Deflandre, B., Žlvađinovic´, M. K., et al. (2010). In vitro simulation of oxic/suboxic diagenesis in an estuarine fluid mud subjected to redox oscillations. *Estuarine, Coastal and Shelf Science*, *88*(2), 279–291. https://doi.org/10.1016/j.ecss.2010.04.003

Adhikari, D., & Yang, Y. (2015). Selective stabilization of aliphatic organic carbon by iron oxide. *Scientific Reports*, *5*(1), 11214. https://doi.org/10.1038/srep11214

Adhikari, D., Zhao, Q., Das, K., Mejia, J., Huang, R., Wang, X., et al. (2017). Dynamics of ferrihydrite-bound organic carbon during microbial Fe reduction. *Geochimica et Cosmochimica Acta*, *212*, 221–233. https://doi.org/10.1016/j.gca.2017.06.017

Aller, R. C. (1998). Mobile deltaic and continental shelf muds as suboxic, fluidized bed reactors. *Marine Chemistry*, *61*(3-4), 143–155. https://doi.org/10.1016/S0304-4203(98)00024-3

Aller, R. C. (2004). Conceptual models of early diagenetic processes: The muddy seafloor as an unsteady, batch reactor. *Journal of Marine Research*, *62*(6), 815–835. https://doi.org/10.1357/0022240042880837

Aller, R. C., & Blair, N. E. (2006). Carbon remineralization in the Amazon-Guianas tropical mobile mudbelt: A sedimentary incinerator. *Continental Shelf Research*, *26*(17-18), 2241–2259. https://doi.org/10.1016/j.csr.2006.07.016

Aller, R. C., Hannides, A., Heilbrun, C., & Panzeca, C. (2004). Coupling of early diagenetic processes and sedimentary dynamics in tropical shelf environments: The Gulf of Papua deltaic complex. *Continental Shelf Research*, *24*(19), 2455–2486. https://doi.org/10.1016/j.csr.2004.07.018

Aller, R. C., Heilbrun, C., Panzeca, C., Zhu, Z., & Baltzer, F. (2004). Coupling between sedimentary dynamics, early diagenetic processes, and biogeochemical cycling in the Amazon-Guianas mobile mud belt: Coastal French Guiana. *Marine Geology*, *208*(2-4), 331–360. https://doi.org/10.1016/j.margeo.2004.04.027

Aller, R. C., Mackin, J. E., Ullman, W. J., & Chen, W. (1985). Early chemical diagenesis, sediment-water solute exchange, and storage of reactive organic matter near the mouth of the Changjiang, East China Sea. *Continental Shelf Research*, *4*(1-2), 227–251. https://doi.org/10.1016/0278-4343(85)90031-7

Audry, S., Blanc, G., Schäfer, J., & Robert, S. (2007). Effect of estuarine sediment resuspension on early diagenesis, sulfide oxidation and dissolved molybdenum and uranium distribution in the Gironde estuary, France. *Chemical Geology*, *238*(3-4), 149–167. https://doi.org/10.1016/j.chemgeo.2006.11.006

Bao, R., Mcintyre, C., Zhao, M., Zhu, C., Kao, S. J., & Eglinton, T. I. (2016). Widespread dispersal and aging of organic carbon in shallow marginal seas. *Geology*, *44*, G37,941–G37,948.

Barber, A., Brandes, J., Leri, A., Lalonde, K., Balind, K., Wirick, S., et al. (2017). Preservation of organic matter in marine sediments by inner-sphere interactions with reactive iron. *Scientific Reports*, *7*(1), 366. https://doi.org/10.1038/s41598-017-00494-0

Benner, R., Fogel, M. L., Sprague, E. K., & Hodson, R. E. (1987). Depletion of ^{13}C in lignin and its implications for stable carbon isotope studies. *Nature*, *329*(6141), 708–710. https://doi.org/10.1038/329708a0

Bergamaschi, B. A., Tsamakis, E., Keil, R. G., Eglinton, T. I., Montluçon, D. B., & Hedges, J. I. (1997). The effect of grain size and surface area on organic matter, lignin and carbohydrate concentration, and molecular compositions in Peru Margin sediments. *Geochimica et Cosmochimica Acta*, *61*(6), 1247–1260. https://doi.org/10.1016/S0016-7037(96)00394-8

Bianchi, T. S., & Allison, M. A. (2009). Large-river delta-front estuaries as natural "recorders" of global environmental change. *Proceedings of the National Academy of Sciences*, *106*(20), 8085–8092. https://doi.org/10.1073/pnas.0812878106

Blair, N. E., & Aller, R. C. (2012). The fate of terrestrial organic carbon in the marine environment. *Annual Review of Marine Science*, *4*(1), 401–423. https://doi.org/10.1146/annurev-marine-120709-142717

Burdige, D. J. (2005). Burial of terrestrial organic matter in marine sediments: A re-assessment. *Global Biogeochemical Cycles*, *19*, GB4011. https://doi.org/10.1029/2004GB002368

Burdige, D. J. (2006). *Geochemistry of Marine Sediments*. New Jersey: Princeton University Press.

Canfield, D. E., Thamdrup, B., & Hansen, J. W. (1993). The anaerobic degradation of organic matter in Danish coastal sediments: Iron reduction, manganese reduction, and sulfate reduction. *Geochimica et Cosmochimica Acta*, *57*(16), 3867–3883. https://doi.org/10.1016/0016-7037(93)90340-3

Chen, C., Dynes, J. J., Wang, J., & Sparks, D. L. (2014). Properties of Fe-organic matter associations via coprecipitation versus adsorption. *Environmental Science & Technology*, *48*(23), 13,751–13,759. https://doi.org/10.1021/es503669u

Chen, C., Kukkadapu, R., & Sparks, D. L. (2015). Influence of coprecipitated organic matter on Fe^{2+} (aq)-catalyzed transformation of ferrihydrite: Implications for carbon dynamics. *Environmental Science & Technology*, *49*(18), 10,927–10,936. https://doi.org/10.1021/acs.est.5b02448

Chin, Y., Traina, S. J., Swank, C. R., & Backhus, D. (1998). Abundance and properties of dissolved organic matter in pore waters of a freshwater wetland. *Limnology and Oceanography*, *43*(6), 1287–1296. https://doi.org/10.4319/lo.1998.43.6.1287

Christl, I., & Kretzschmar, R. (2007). C-1s NEXAFS spectroscopy reveals chemical fractionation of humic acid by cation-induced coagulation. *Environmental Science & Technology*, *41*(6), 1915–1920. https://doi.org/10.1021/es062141s

DeMaster, D. J., Mckee, B. A., Nittrouer, C. A., Qian, J., & Cheng, G. (1985). Rates of sediment accumulation and particle reworking based on radiochemical measurements from continental shelf deposits in the East China Sea. *Continental Shelf Research*, *4*(1-2), 143–158. https://doi.org/10.1016/0278-4343(85)90026-3

Dittmar, T., & Lara, R. J. (2001). Molecular evidence for lignin degradation in sulfate-reducing mangrove sediments (Amazônia, Brazil). *Geochimica et Cosmochimica Acta*, *65*(9), 1417–1428. https://doi.org/10.1016/S0016-7037(00)00619-0

Doetterl, S., Berhe, A. A., Nadeu, E., Wang, Z., Sommer, M., & Fiener, P. (2016). Erosion, deposition and soil carbon: A review of process-level controls, experimental tools and models to address C cycling in dynamic landscapes. *Earth-Science Reviews*, *154*, 102–122. https://doi.org/10.1016/j.earscirev.2015.12.005

Eglinton, T. I. (2012). A rusty carbon sink. *Nature*, *483*(7388), 165–166. https://doi.org/10.1038/483165a

Eusterhues, K., Hädrich, A., Neidhardt, J., Küsel, K., Keller, T. F., Jandt, K. D., & Totsche, K. U. (2014). Reduction of ferrihydrite with adsorbed and coprecipitated organic matter: Microbial reduction by Geobacter bremensis vs. abiotic reduction by Na-dithionite. *Biogeosciences*, *11*(4), 6039–6067. https://doi.org/10.5194/bgd-11-6039-2014

Ge, C., Zhang, W., Dong, C., Wang, F., Feng, H., Qu, J., & Yu, L. (2017). Tracing sediment erosion in the Yangtze River subaqueous delta using magnetic methods. *Journal of Geophysical Research: Earth Surface*, *122*, 2064–2078. https://doi.org/10.1002/2017JF004403

Goñi, M. A., & Hedges, J. I. (1995). Sources and reactivities of marine-derived organic matter in coastal sediments as determined by alkaline Cuo oxidation. *Geochimica et Cosmochimica Acta*, *59*(14), 2965–2981. https://doi.org/10.1016/0016-7037(95)00188-3

Guo, Z., Yang, Z., Fan, D., & Pan, Y. (2003). Seasonal variation of sedimentation in the Changjiang estuary mud area. *Journal of Geographical Sciences*, *13*, 348–354.

Hedges, J. I., Blanchette, R. A., Weliky, K., & Devol, A. H. (1988). Effects of fungal degradation on the cuo oxidation products of lignin: A controlled laboratory study. *Geochimica et Cosmochimica Acta*, *52*(11), 2717–2726. https://doi.org/10.1016/0016-7037(88)90040-3

Hedges, J. I., & Ertel, J. R. (1982). Characterization of lignin by gas capillary chromatography of cupric oxide oxidation products. *Analytical Chemistry*, *54*(2), 174–178. https://doi.org/10.1021/ac00239a007

Hedges, J. I., & Keil, R. G. (1995). Sedimentary organic matter preservation: An assessment and speculative synthesis. *Marine Chemistry*, *49*, 123–126.

Hedges, J. I., & Mann, D. C. (1979). The characterization of plant tissues by their lignin oxidation products. *Geochimica et Cosmochimica Acta*, *43*(11), 1803–1807. https://doi.org/10.1016/0016-7037(79)90028-0

Hernes, P. J., Kaiser, K., Dyda, R. Y., & Cerli, C. (2013). Molecular trickery in soil organic matter: Hidden lignin. *Environmental Science & Technology*, *47*(16), 9077–9085. https://doi.org/10.1021/es401019n

Houel, S., Louchouarn, P., Lucotte, M., Canuel, R., & Ghaleb, B. (2006). Translocation of soil organic matter following reservoir impoundment in boreal systems: Implications for in situ productivity. *Limnology and Oceanography*, *51*(3), 1497–1513. https://doi.org/10.4319/lo.2006.51.3.1497

Hyacinthe, C., Bonneville, S., & Van Cappellen, P. (2006). Reactive iron in sediments: Chemical versus microbial extractions. *Geochimica et Cosmochimica Acta*, *70*(16), 4166–4180. https://doi.org/10.1016/j.gca.2006.05.018

James, F. (2004). MINUIT tutorial—Function minimization, in: Proceedings of the 1972 CERN computing and data processing school, Pertisau, Austria, 10–24. September, 1972, CERN, Switzerland, 72–21.

Jaynes, W. F., & Bigham, J. M. (1986). Concentration of iron oxides from soil clays by density gradient centrifugation. *Soil Science Society of America Journal*, *50*(6), 1633–1639. https://doi.org/10.2136/sssaj1986.03615995005000060049x

Jilbert, T., Asmala, E., Schröder, C., Tiihonen, R., Myllykangas, J. P., Virtasalo, J. J., et al. (2018). Impacts of flocculation on the distribution and diagenesis of iron in boreal estuarine sediments. *Biogeosciences*, *12*, 1519–1522.

Kaiser, K., & Guggenberger, G. (2000). The role of DOM sorption to mineral surfaces in the preservation of organic matter in soils. *Organic Geochemistry*, *31*(7-8), 711–725. https://doi.org/10.1016/S0146-6380(00)00046-2

Keil, R. G., & Mayer, L. M. (2014). Mineral matrices and organic matter. *Treatise on Geochemistry*, *76*, 337–359.

Klingelhöfer, G., Morris, R. V., Bernhardt, B., Rodionov, D., de Souza, P. A. Jr., Squyres, S. W., et al. (2003). Athena MIMOS II Mössbauer spectrometer investigation. *Journal of Geophysical Research*, *108*(E12), 8067. https://doi.org/10.1029/2003JE002138

Lalonde, K., Mucci, A., Ouellet, A., & Gélinas, Y. (2012). Preservation of organic matter in sediments promoted by iron. *Nature*, *483*(7388), 198–200. https://doi.org/10.1038/nature10855

Lee, H. J., & Chao, S. Y. (2003). A climatological description of circulation in and around the East China Sea. *Deep Sea Research Part II Topical Studies in Oceanography*, *50*(6-7), 1065–1084. https://doi.org/10.1016/S0967-0645(03)00010-9

Li, D., Yao, P., Bianchi, T. S., Zhang, T., Zhao, B., Pan, H., et al. (2014). Organic carbon cycling in sediments of the Changjiang Estuary and adjacent shelf: Implication for the influence of three Gorges Dam. *Journal of Marine Systems*, *139*, 409–419. https://doi.org/10.1016/j.jmarsys.2014.08.009

Li, D. J., Wu, Y., Zhang, J., Liang, J., & Huang, D. J. (2002). Oxygen depletion off the Changjiang (Yangtze River) Estuary. *Science in China*, *45*(12), 1137–1146. https://doi.org/10.1360/02yd9110

Li, X., Bianchi, T. S., Yang, Z., Osterman, L. E., Allison, M. A., Dimarco, S. F., & Yang, G. (2011). Historical trends of hypoxia in Changjiang River estuary: Applications of chemical biomarkers and microfossils. *Journal of Marine Systems*, *86*(3-4), 57–68. https://doi.org/10.1016/j.jmarsys.2011.02.003

Lin, S., Hsieh, I. J., Huang, K. M., & Wang, C. H. (2002). Influence of the Yangtze River and grain size on the spatial variations of heavy metals and organic carbon in the East China Sea continental shelf sediments. *Chemical Geology*, *182*(2-4), 377–394. https://doi.org/10.1016/S0009-2541(01)00331-X

Linkhorst, A., Dittmar, T., & Waska, H. (2017). Molecularfractionation of dissolved organic matter in a shallow subterranean estuary: The role of the iron curtain. *Environmental Science & Technology*, *51*(3), 1312–1320. https://doi.org/10.1021/acs.est.6b03608

Liu, J., Zhu, M. X., Yang, G. P., Shi, X. N., & Yang, R. J. (2014). Quick sulfide buffering in inner shelf sediments of the East China Sea impacted by eutrophication. *Environmental Earth Sciences*, *71*(1), 465–473. https://doi.org/10.1007/s12665-013-2454-4

Liu, J. P., Li, A. C., Xu, K. H., Velozzi, D. M., Yang, Z. S., Milliman, J. D., & DeMaster, D. J. (2006). Sedimentary features of the Yangtze river-derived along-shelf clinoform deposit in the East China Sea. *Continental Shelf Research*, *26*(17-18), 2141–2156. https://doi.org/10.1016/j.csr.2006.07.013

Liu, J. P., Xu, K. H., Li, A. C., Milliman, J. D., Velozzi, D. M., Xiao, S. B., & Yang, Z. S. (2007). Flux and fate of Yangtze River sediment delivered to the East China Sea. *Geomorphology*, *85*(3-4), 208–224. https://doi.org/10.1016/j.geomorph.2006.03.023

Liu, K. K., Peng, T. H., Shaw, P. T., & Shiah, F. K. (2003). Circulation and biogeochemical processes in the East China Sea and the vicinity of Taiwan: An overview and a brief synthesis. *Deep Sea Research Part II Topical Studies in Oceanography*, *50*(6-7), 1055–1064. https://doi.org/10.1016/S0967-0645(03)00009-2

Louchouarn, P., Lucotte, M., & Farella, N. (1999). Historical and geographical variations of sources and transport of terrigenous organic matter within a large-scale coastal environment. *Organic Geochemistry*, *30*(7), 675–699. https://doi.org/10.1016/S0146-6380(99)00019-4

Lv, J., Zhang, S., Wang, S., Luo, L., Cao, D., & Christie, P. (2016). Molecular-scale investigation with ESI-FT-ICR-MS on fractionation of dissolved organic matter induced by adsorption on iron oxyhydroxides. *Environmental Science & Technology*, *50*(5), 2328–2336. https://doi.org/10.1021/acs.est.5b04996

Ma, W. W., Zhu, M. X., Yang, G. P., & Li, T. (2018). Iron geochemistry and organic carbon preservation by iron (oxyhydr) oxides in surface sediments of the East China Sea and the south Yellow Sea. *Journal of Marine Systems*, *178*, 62–74. https://doi.org/10.1016/j.jmarsys.2017.10.009

Mayer, L. M. (1994). Relationships between mineral surfaces and organic carbon concentrations in soils and sediments. *Chemical Geology*, *114*(3-4), 347–363. https://doi.org/10.1016/0009-2541(94)90063-9

McKee, B. A., Aller, R. C., Allison, M. A., Bianchi, T. S., & Kineke, G. C. (2004). Transport and transformation of dissolved and particulate materials on continental margins influenced by major rivers: Benthic boundary layer and seabed processes. *Continental Shelf Research*, *24*(7-8), 899–926. https://doi.org/10.1016/j.csr.2004.02.009

Mehra, O. P., & Jackson, M. L. (1958). Iron oxide removal from soils and clays by a dithionite-citrate system buffered with sodium bicarbonate. In *Proceedings 7th National Conference Clays* (Vol. 5, pp. 317–327). London: Pergamon Press.

Meyers, P. A. (1997). Organic geochemical proxies of paleoceanographic, paleolimnologic, and paleoclimatic processes. *Organic Geochemistry*, *27*(5-6), 213–250. https://doi.org/10.1016/S0146-6380(97)00049-1

Milliman, J. D., & Farnsworth, K. L. (2011). *River discharge to the coastal ocean-a global synthesis*. Cambridge: Cambridge University Press. https://doi.org/10.1017/CBO9780511781247

Milliman, J. D., Shen, H. T., Yang, Z. S., & Mead, R. H. (1985). Transport and deposition of river sediment in the Changjiang Estuary and adjacent continental shelf. *Continental Shelf Research*, *4*(1-2), 37–45. https://doi.org/10.1016/0278-4343(85)90020-2

Poulton, S. W., & Raiswell, R. (2005). Chemical and physical characteristics of iron oxides in riverine and glacial meltwater sediments. *Chemical Geology*, *218*(3-4), 203–221. https://doi.org/10.1016/j.chemgeo.2005.01.007

Qin, Y., Zhao, Y., Chen, L., & Zhao, S. (1996). *Geology of the East China Sea*. Beijing: China Sci. Press.

Raiswell, R. (2011). Iron transport from the continents to the open ocean: The aging-rejuvenation cycle. *Elements*, *7*(2), 101–106. https://doi.org/10.2113/gselements.7.2.101

Riedel, T., Biester, H., & Dittmar, T. (2012). Molecular fractionation of dissolved organic matter with metal salts. *Environmental Science & Technology*, *46*(8), 4419–4426. https://doi.org/10.1021/es203901u

Riedel, T., Zak, D., Biester, H., & Dittmar, T. (2013). Iron traps terrestrially derived dissolved organic matter at redox interfaces. *Proceedings of the National Academy of Sciences*, *110*(25), 10,101–10,105. https://doi.org/10.1073/pnas.1221487110

Roden, E. E. (2004). Analysis of long-term bacterial vs. chemical Fe (III) oxide reduction kinetics. *Geochimica et Cosmochimica Acta*, *68*(15), 3205–3216. https://doi.org/10.1016/j.gca.2004.03.028

Salvadó, J. A., Tesi, T., Andersson, A., Ingri, J., Dudarev, O. V., Semiletov, I. P., & Gustafsson, Ö. (2015). Organic carbon remobilized from thawing permafrost is resequestered by reactive iron on the Eurasian Arctic shelf. *Geophysical Research Letters*, *42*, 8122–8130. https://doi.org/10.1002/2015GL066058

Shields, M. R., Bianchi, T. S., Gélinas, Y., Allison, M. A., & Twilley, R. R. (2016). Enhanced terrestrial carbon preservation promoted by reactive iron in deltaic sediments. *Geophysical Research Letters*, *43*, 1149–1157. https://doi.org/10.1002/2015GL067388

Sirois, M., Couturier, M., Barber, A., Gélinas, Y., & Chaillou, G. (2018). Interactions between iron and organic carbon in a sandy beach subterranean estuary. *Marine Chemistry*, *202*, 86–96. https://doi.org/10.1016/j.marchem.2018.02.004

Stucki, J. W., Lee, K., Goodman, B. A., & Kostka, J. E. (2007). Effects of in situ, biostimulation on iron mineral speciation in a sub-surface soil. *Geochimica et Cosmochimica Acta*, *71*(4), 835–843. https://doi.org/10.1016/j.gca.2006.11.023

Thullner, M., Dale, A. W., & Regnier, P. (2009). Global-scale quantification of mineralization pathways in marine sediments: A reaction-transport modeling approach. *Geochemistry, Geophysics, Geosystems*, *11*, Q10012. https://doi.org/10.1029/2009GC002484

Torn, M. S., Trumbore, S. E., Chadwick, O. A., Vitousek, P. M., & Hendricks, D. M. (1997). Mineral control of soil organic carbon storage and turnover. *Nature*, *389*(6647), 170–173. https://doi.org/10.1038/38260

Van der Voort, T. S., Mannu, U., Blattmann, T. M., Bao, R., Zhao, M., & Eglinton, T. I. (2018). Deconvolving the fate of carbon in coastal sediments. *Geophysical Research Letters*, *45*, 4134–4142. https://doi.org/10.1029/2018GL077009

Wagai, R., & Mayer, L. M. (2007). Sorptive stabilization of organic matter in soils by hydrous iron oxides. *Geochimica et Cosmochimica Acta*, *71*(1), 25–35. https://doi.org/10.1016/j.gca.2006.08.047

Wang, J., Yao, P., Bianchi, T. S., Li, D., Zhao, B., Cui, X. Q., et al. (2015). The effect of particle density on the sources, distribution, and degradation of sedimentary organic carbon in the Changjiang Estuary and adjacent shelf. *Chemical Geology*, *402*(9), 52–67.

Wang, X., Ma, H., Li, R., Song, Z., & Wu, J. (2012). Seasonal fluxes and source variation of organic carbon transported by two major Chinese Rivers: The Yellow River and Changjiang (Yangtze) River. *Global Biogeochemical Cycles*, *26*, GB2025. https://doi.org/10.1029/2011GB004130

Wang, Y., Wang, H., He, J. S., & Feng, X. (2017). Iron-mediated soil carbon response to water-table decline in an alpine wetland. *Nature Communications*, *8*, 15972.

Wells, M. L., Price, N. M., & Bruland, K. W. (1995). Iron chemistry in seawater and its relationship to phytoplankton: A workshop report. *Marine Chemistry*, *48*(2), 157–182. https://doi.org/10.1016/0304-4203(94)00055-I

Wu, Y., Zhang, J., Liu, S. M., Zhang, Z. F., Yao, Q. Z., Hong, G. H., & Cooper, L. (2007). Sources and distribution of carbon within the Yangtze river system. *Estuarine, Coastal and Shelf Science*, *71*(1-2), 13–25. https://doi.org/10.1016/j.ecss.2006.08.016

Xu, B., Bianchi, T. S., Allison, M. A., Dimova, N. T., Wang, H., Zhang, L., et al. (2015). Using multi-radiotracer techniques to better understand sedimentary dynamics of reworked muds in the Changjiang River Estuary and inner shelf of East China Sea. *Marine Geology*, *370*, 76–86. https://doi.org/10.1016/j.margeo.2015.10.006

Yao, P., Yu, Z., Bianchi, T. S., Guo, Z., Zhao, M., Knappy, C. S., et al. (2015). A multiproxy analysis of sedimentary organic carbon in the changjiang estuary and adjacent shelf. *Journal of Geophysical Research: Biogeosciences*, *120*, 1407–1429. https://doi.org/10.1002/2014JG002831

Yao, P., Zhao, B., Bianchi, T. S., Guo, Z., Zhao, M., Li, D., et al. (2014). Remineralization of sedimentary organic carbon in mud deposits of the Changjiang Estuary and adjacent shelf: Implications for carbon preservation and authigenic mineral formation. *Continental Shelf Research*, *91*, 1–11. https://doi.org/10.1016/j.csr.2014.08.010

Zhang, J., Liu, S. M., Ren, J. L., Wu, Y., & Zhang, G. L. (2007). Nutrient gradients from the eutrophic Changjiang (Yangtze River) Estuary to the oligotrophic Kuroshio waters and re-evaluation of budgets for the East China Sea Shelf. *Progress in Oceanography*, *74*(4), 449–478. https://doi.org/10.1016/j.pocean.2007.04.019

Zhang, J., Wu, Y., Jennerjahn, T. C., Ittekkot, V., & He, Q. (2007). Distribution of organic matter in the Changjiang (Yangtze River) Estuary and their stable carbon and nitrogen isotopic ratios: Implications for source discrimination and sedimentary dynamics. *Marine Chemistry*, *106*(1-2), 111–126. https://doi.org/10.1016/j.marchem.2007.02.003

Zhao, B., Yao, P., Bianchi, T. S., Arellano, A. R., Wang, X. C., Yang, J. B., et al. (2018). The remineralization of sedimentary organic carbon in different sedimentary regimes of the Yellow and East China Seas. *Chemical Geology*, *495*, 104–117. https://doi.org/10.1016/j.chemgeo.2018.08.012

Zhao, B., Yao, P., Bianchi, T. S., Xu, Y., Liu, H., Mi, T., et al. (2017). Early diagenesis and authigenic mineral formation in mobile muds of the Changjiang Estuary and adjacent shelf. *Journal of Marine Systems*, *172*, 64–74. https://doi.org/10.1016/j.jmarsys.2017.03.001

Zhao, J., Feng, X., Shi, X., Bai, Y., Yu, X., Shi, X., et al. (2015). Sedimentary organic and inorganic records of eutrophication and hypoxia in and off the Changjiang Estuary over the last century. *Marine Pollution Bulletin*, *99*(1-2), 76–84. https://doi.org/10.1016/j.marpolbul.2015.07.060

Zhu, J., Zhu, Z., Lin, J., Wu, H., & Zhang, J. (2015). Distribution of hypoxia and pycnocline off the Changjiang Estuary, China. *Journal of Marine Systems*, *154*, 28–40.

Zhu, M. X., Chen, K., Yang, G., Fan, D., & Li, T. (2016). Sulfur and iron diagenesis in temperate unsteady sediments of the East China Sea inner shelf and a comparison with tropical mobile mud belts (MMBs). *Journal of Geophysical Research: Biogeosciences*, *121*, 2811–2828. https://doi.org/10.1002/2016JG003391

Zhu, M. X., Hao, X. C., Shi, X. N., Yang, G. P., & Li, T. (2012). Speciation and spatial distribution of solid-phase iron in surface sediments of the East China Sea continental shelf. *Applied Geochemistry*, *27*(4), 892–905. https://doi.org/10.1016/j.apgeochem.2012.01.004